Surrogate Affine Approximation based Co-optimization of Transactive Flexibility, Uncertainty, and Energy

Hongxing Ye, *Senior Member, IEEE*

***Abstract*—This study presents an approach to co-optimization of transactive flexibility, energy, and optimal injection-range of Variable Energy Resource (VER). Flexibility receives immense attention, as it is the essential resource to accommodate VERs in modern power systems. With a novel concept of transactive flexibility, the proposed approach proactively positions the flexible resources and optimizes the demand of flexibility. A Surrogate Affine Approximation (SAA) method is proposed to solve the problem with variable infinite-constraint range in polynomial time. It is shown that SAA is more optimistic than the traditional affine policy in power literature. The SAA method is also applicable to the search for secure injection-range of VER, which is often heuristically determined in industry given the latest system information. In practice, VER generation beyond the secure injection-range has to be curtailed, even if its cost is lower than the marginal price. The proposed technique helps accommodate more VERs securely and economically by increasing secure injection-range. The model and the solution approach are illustrated in the six-bus system and IEEE 118-bus system.**

***Index Terms*—Flexibility and Uncertainty, Secure Injection-Range, Dispatchable Renewables, Surrogate Optimization, Affine Policy, Electricity Market**

NOMENCLATURE

Indices

i	index of fully-controllable unit
l	index of transmission line
n	index of bus/aggregated VER generator
t	index of time

Sets and notations

$C(\cdot)$	cost function. $C_c(\cdot)$ for generation cost of fully controllable generator; $C_v(\cdot)$ for cost of VER generation; $C_d(\cdot)$ for the benefit of load; $C_f(\cdot)$ for the benefit of upward/downward flexibility
$\mathrm{diag}(\cdot)$	diagonal matrix whose diagonal entries are elements of vector $\cdot$
$\mathcal{G}(n)$	set of units located at bus n
$\mathcal{J}$	set of rows in (4d)
$\max(\cdot,\cdot)$	element-wise maximum operator
$\mathcal{N}_b$	set of buses
$\mathcal{N}_g$	set of generators
$\mathcal{N}_l$	set of lines
$\mathbb{R}^x$	set of real x-vectors
$\mathbb{R}^{x\times y}$	set of real $x \times y$ matrices
$\mathcal{T}$	set of time intervals
$\mathcal{U}(\boldsymbol{u})$	uncertainty set, a function of flexibility $\boldsymbol{u}$
$\tilde{\mathcal{U}}$	surrogate uncertainty set (constant)

Constants

$\boldsymbol{A}, \boldsymbol{b}$	abstract matrix and vector for constraint (2a)-(2d)
$\boldsymbol{B}, \boldsymbol{C}, \boldsymbol{E}, \boldsymbol{d}$	abstract matrices and vector for constraint (3a)-(3d)
$\boldsymbol{c}, \boldsymbol{f}$	abstract coefficient vectors for $\boldsymbol{x}$ and $\boldsymbol{u}$
$\boldsymbol{F}, \boldsymbol{H}, \boldsymbol{h}$	abstract matrices and vector for constraint (2e)-(2f)
$\bar{F}_l$	branch flow limit
N_b	number of buses
N_g	number of units
N_l	number of transmission lines
N_r	number of rows in (4d)
$P_i^{\min}, P_i^{\max}$	minimum and maximum generation outputs
$R_i^{\text{up}}, R_i^{\text{down}}$	unit ramping up/down limits (MW/minute)
T	number of time intervals
δ	timespan of one interval
$\Gamma_{l,n}$	shift factor for line l and bus n

Variables

D_n	load demand at bus n
$\boldsymbol{G}$	generation adjustment matrix, $\boldsymbol{G} \in \mathbb{R}^{N_g\times N_b}$
$\tilde{\boldsymbol{G}}$	surrogate generation adjustment matrix, $\tilde{\boldsymbol{G}} \in \mathbb{R}^{N_g\times N_b}$
$J_{\text{SAA}}, J_{\text{AP}}$	optimal values of problem (SAA-P) and (TAP-P)
P_i	output of fully controllable generator i
$\hat{P}_i(\boldsymbol{v})$	re-dispatch of fully controllable generator i, a function of $\boldsymbol{v}$
$P_{i,t}$	output of fully controllable generator i at time t in the extended multi-period model
$\boldsymbol{s}(\boldsymbol{u}^{\text{LB}}, \boldsymbol{u}^{\text{UB}})$	surrogate function $\boldsymbol{s}(\boldsymbol{u}^{\text{LB}}, \boldsymbol{u}^{\text{UB}}) : \mathbb{R}^{2N_b} \to \mathbb{R}^{2N_b}$
$\boldsymbol{u}^{\text{LB}}, \boldsymbol{u}^{\text{UB}}$	downward and upward flexibility (allowed downward and upward deviations from VER's perspective), $\boldsymbol{u}^{\text{LB}} \in \mathbb{R}^{N_b}, \boldsymbol{u}^{\text{UB}} \in \mathbb{R}^{N_b}$
$\boldsymbol{u}$	$\boldsymbol{u} = [(\boldsymbol{u}^{\text{LB}})^\top, (\boldsymbol{u}^{\text{UB}})]^\top$
$\boldsymbol{U}^{\text{LB}}, \boldsymbol{U}^{\text{UB}}$	matrix $\mathrm{diag}(\boldsymbol{u}^{\text{LB}})$ and $\mathrm{diag}(\boldsymbol{u}^{\text{UB}})$

This work is supported in part by the U.S. National Science Foundation Project Number ECCS-1711217 and Cleveland State University Faculty Research & Development Program. H. Ye is with the Cleveland State University, Cleveland, OH 44115, USA. (e-mail: h.ye@csuohio.edu).

Digital Object Identifier 10.1109/TPWRS.2018.2790170

$U_n^{\text{LB}}, U_n^{\text{UB}}$	upward and downward flexibility (allowed downward and upward deviation of VER output)
$\boldsymbol{v}$	realized VER output vector, $\boldsymbol{v} \in \mathbb{R}^{N_b}$
V_n	realized VER power output
V_n^s	scheduled VER power output
$\underline{V}_n, \bar{V}_n$	lower and upper bound of allowed VER power injection at the second stage, $[\underline{V}_n, \bar{V}_n]$ is the optimal injection-range of VER n
V_n^f	forecast expectation of VER output
$\underline{V}_n^f$	forecast lower bound of VER output
$\boldsymbol{x}$	abstract vector denoting generation dispatch, VER output, and load demand
$\boldsymbol{y}(\boldsymbol{\epsilon})$	corrective action, a function of $\boldsymbol{\epsilon}$
$\hat{\boldsymbol{y}}(\boldsymbol{\epsilon})$	surrogate corrective action, a function of $\boldsymbol{\epsilon}$
$\epsilon_n, \boldsymbol{\epsilon}$	uncertainty at bus n and uncertainty vector, $\boldsymbol{\epsilon} \in \mathbb{R}^{N_b}$
$\boldsymbol{\pi}, \boldsymbol{\pi}^{\text{LB}}, \boldsymbol{\pi}^{\text{UB}}$	non-negative matrix of auxiliary multipliers

I. Introduction

VARIABLE energy resources (VERs), such as solar and wind power, have experienced rapid growth in the last decades. In the U.S., wind and solar capacity have increased by 100% and 900%, respectively, between 2009 and 2015 [1]. At the end of 2016, the solar and utility-scale wind generation capacity reach 42.4GW and 81.3GW, respectively. Compared with traditional fossil fuel-fired units, VER generators are not fully controllable. They bring more variability and uncertainty in the power system.

In the U.S., an important task of the Independent System Operator (ISO) or Regional Transmission Organization (RTO) is to make the short-term generation schedule, which is to supply the load respecting physical limits and security constraints. In the power community, the Unit Commitment (UC) problem is defined as finding the optimal unit ON/OFF status, and the Economic Dispatch (ED) is to find the most cost-efficient generation output schedule [2], [3]. When the penetration of VERs reaches the certain level, ISOs/RTOs have to mitigate the adverse impacts of the variability and uncertainty from VER generators. The flexible resources, such as natural gas-fired unit with large ramping rate, demand response, and energy storage, are the ideal assets to achieve this goal by providing flexibility.

VER generators are not fully controllable, and their generations are often treated as uncertain parameters. Thus, with the rapid growth of VERs, the scheduling problems considering uncertainty become active research topics in modern power systems. In the literature, two of the candidate approaches to handling uncertainties are stochastic programming and robust optimization [4]–[8]. Scenario-based stochastic programming approaches often model a number of scenarios to get the cost expectation and reserve flexible resources by utilizing Probability Density Function (PDF). However, due to the computational intractability, many approaches only consider a small portion of scenarios using sample-reduction techniques. Recently, the chance-constrained stochastic approach is also employed to solve optimal power flow problems [9]. In robust optimization-based approaches, probability information is not required and its solution is supposed to be immune to any uncertainty in the predefined uncertainty set. It often requires efforts in solving the NP-hard max-min problems to obtain a robust and optimal solution.

In the real-time market, ISOs/RTOs are supposed to obtain the optimal solution within several minutes, given the latest available information, such as load and VER forecast output. To address the computational challenge, researchers have introduced affine policy in UC and ED problems [9]–[11]. Affine policy can be traced back to 1950s in the chance-constrained stochastic programming [12]. The strict affine policy helps make the problem tractable. In industry, a similar principle is widely applied in Automatic Generation Control (AGC) [13] that is designed to balance the system frequency and the scheduled interchange in seconds. The main difference is that the participation factors are heuristically determined in AGC.

Flexibility has received many attentions in recent years, such as [14]–[21]. Flexibility is considered as part of the generation expansion problem [14], [16], [17]. A metric for flexibility is further introduced, and profits of flexibility providers are analyzed in [17]. However, the inherent stochastic nature of renewable is not considered. In [18], [19], the authors present approaches to utilizing the renewables as flexible resources. [20] presents a framework for coordinating available reserves using tie-line in multi-area. This author, Ge, Shahidehpour, and Li's previous work presents a pricing scheme for flexibility in robust optimization [21], [22].

Realizing the increasing value of flexibility in power systems with deep VER penetration, several ISOs/RTOs have taken actions to secure more flexible resources. For example, CAISO has increased the reserve requirements, and both CAISO and MISO have introduced ramping products in the electricity market. At the same time, as flexibility in the system is finite, renewable energy spillage often occurs in the real-time market. Thus, ISO-NE proposes the DO-NOT-EXCEED (DNE) limit in the real-time market [23]. It gives clear dispatch signal for each VER generator, which is instructed to curtail the VER generation beyond the DNE limit. Recently, researchers present interesting results on this topic by maximizing the norm of range vector and utilizing historical data [24], [25].

While the terminology "flexibility" could have many definitions, in this work, *flexibility is defined as the range of power-injection-change that the system can accommodate using available flexible resources within the specified time*. The flexible resources can be either from the generation side or from Load Serving Entity (LSE) side. Furthermore, they can be delivered to the desired destination respecting transmission constraints. In this paper, the upward (downward) flexibility is defined as the maximum accommodable power-injection-change in upward (downward) direction.

Most literature of flexibility is on the supply side of flexible resource that is often secured by the system operator based on some heuristic requirements. This work introduces a novel concept, transactive flexibility, to optimize both demand and supply of flexibility. It enables the owners of flexible resource and demanders of flexibility to manage flexibility actively.

The demander of flexibility is allowed to procure flexibility so that she is able to manage the uncertainty or variation of power injection considering the benefit. The proposed model optimally positions flexible resource and manages flexibility demand via a two-sided market. The transmission reserves are implicitly held so that deliverability of flexible resources is guaranteed. Energy is often transactive, i.e., it can be bought and sold in the electricity market. However, flexible resources, such as ramping product, can only be sold in the existing markets. In the existing literature, flexibility providers are entitled to credits for reserving ramping capability. This author, Ge, Shahidehpour, and Li's previous research [22] further proposes to allocate the flexibility cost to the uncertainty source based on Uncertainty Marginal Price (UMP) following a cost causation principle. The uncertainty source is thus inclined to reduce the uncertainty level.

When flexibility has become increasingly valuable, three questions remain open: 1) how to determine the flexibility amount while keeping ISO/RTO independent; 2) how to allocate flexibility to demander cost-effectively; 3) how to handle the high flexibility demand when the flexible resource is scarce. To address these problems, this paper proposes a co-optimization model where flexibility is treated as a commodity, and a general polynomial solution method. In the proposed model, flexibility can be bought as well as sold. The VER's procurement of flexibility is equivalent to selling uncertainty at a negative price. To the author's best knowledge, this is the first time to introduce the concept of transactive flexibility. Thus, this work mainly focuses on the new co-optimization model and the new solution methodology. The reader is referred to [22] for the pricing schemes. The contributions of this paper are summarized as follows.

1) This paper proposes a new co-optimization model to maximize the total social welfare. A concept, transactive flexibility, is proposed. The model co-optimizes flexibility and energy keeping ISO/RTO independent. System security and economic efficiency are guaranteed. The model will motivate VER to be an autonomous uncertainty mitigator and flexibility demander. The VERs submit the flexibility bid (either zero or positive) so that resources are proactively positioned for more VER integrations. Any VER generations within an optimally determined injection-range can be injected into the grid. Even with zero flexibility bid, it is still possible to find an ED to accommodate more VERs, when a multiplicity of ED occurs.
2) A general Surrogate Affine Approximation (SAA) method is proposed to solve the problem that includes decision variables of infinite-constraint range. It is computationally tractable. By solving one Linear Programming (LP) or Quadratic Programming (QP) problem, one can attain the optimal solution in the proposed approach. It is proved that the optimality of the SAA is never worse than that of the traditional affine policy in power literature. In many circumstances, the SAA method finds a better solution.

   The SAA method is also applicable to the DNE-limit search, which was once regarded as a computationally intractable nonlinear problem. Heuristic methods are often employed to solve it [23]. The SAA method can even find better solutions by solving one LP problem. It helps integrate more VERs.

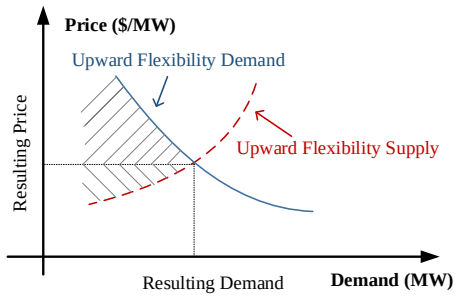

Fig. 1. An illustrative intersection of demand and supply curve for upward flexibility in a system without network congestion. The uncertainty source submits demand curve. The shadow area is the social surplus.

The rest of this paper is organized as follows. In Section II, the co-optimization model is developed with transactive flexibility and uncertainty. The SAA method is presented in Section III. Section IV illustrates the model and solution approach using a simple six-bus system and a modified 118-bus system. Section V concludes this paper.

II. Co-optimization of Transactive Flexibility, Uncertainty, and Energy

The flexibility demand has been increasing significantly with the growing VER penetration in power systems. In many circumstances, flexibility is the scarce resource, that may be even more expensive than energy [27]. To optimally and cost-effectively position flexible resource, this paper presents a model with transactive flexibility, which can be sold by the supplier, and bought by the demander. Flexibility can be either upward or downward. Fig. 1 illustratively depicts an intersection [1] of the demand and supply curve for the upward flexibility. The intersection is the optimal point, which yields the resulting value of price and amount of flexibility. The shadow area is the social surplus. This paper focuses on a new model and solution methodologies. In the proposed model, the flexibility consumer, such as VER, bids for flexibility, so that she can use it for uncertainty accommodation or ramping following. In the meantime, the flexible resource owner gets paid for providing flexibility. The proposed market clearing model follows a cost causation principle. It provides an option to address the challenge of cost allocation and resource deficiency for flexibility. On the other hand, the system operator remains independent in this model.

Similar to stochastic/robust literature, VER generators at the same bus are aggregated as a single one. For simplicity, a single-period ED is considered here in the real-time market. An extension to multi-period ED will be briefly discussed later. Let n denote the bus index; Let V_n^s denote the scheduled VER output; let U_n^{LB} and U_n^{UB} denote the allowable downward

[1] Fig. 1 is used to illustrate the basic idea, and the intersection may be more complicated when the line congestion exists in the system

and upward deviation, respectively; Let V_n denote the realized VER output. Any realized VER output

$$V_n \in [V_n^s - U_n^{\text{LB}}, V_n^s + U_n^{\text{UB}}], \forall n \in \mathcal{N}_b$$

can be injected into the grid. This work considers a new two-stage model to maximize the social welfare, where flexible resources are to be *proactively* positioned at the first stage, and they are used to accommodate uncertainties at the second stage. It is so called "wait-and-see" process. When the scheduled output V_n^s, and allowable deviation for VER are determined, U_n^{LB} and U_n^{UB} are viewed as the largest downward and upward uncertainty at bus n by the system operator. If these uncertainties can always be accommodated by deliverable flexible resource, it is defined in this work that the system has the downward flexibility of U_n^{LB}, and the upward flexibility of U_n^{UB} at bus n. In the proposed model, VER generator is allowed to procure flexibility at the first stage, so that it could inject more energy (i.e., larger injection-range) into the grid at the second stage when uncertainty is realized.

The scheduled VER output $V_{n,t}^s$ respects

$$V_n^s \le V_n^f, \quad V_n^s - \underline{V}_n^f \le U_n^{\text{LB}}, \ \forall n \in \mathcal{N}_b,$$

where V_n^f and $\underline{V}_n^f$ are the forecast expectation, and the forecast lower bound of VER output, respectively. The above equations guarantee that VER output can always be accommodated.

In the proposed co-optimization model, the objective is to minimize the total cost [2] (i.e., the negative of social welfare), which includes cost of energy, benefit of load, and benefit of the injection-range for VER generators. Similar to ramping products [30], [31], the proposed model optimizes the base-case cost. Let $C_c(\cdot)$ and $C_v(\cdot)$ denote cost functions of the conventional generation and VER generation respectively. Let $C_f(\cdot)$ and $C_d(\cdot)$ denote benefit functions of flexibility and load respectively. Then, the objective function of co-optimization ED model is formulated as

$$\min \left(\begin{array}{l} \sum_i C_c(P_i) + \sum_n C_v(V_n^s) \\ -\sum_n C_d(D_n) - \sum_n C_f(U_n^{\text{LB}}, U_n^{\text{UB}}) \end{array} \right) \tag{1}$$

It is subject to

$$\sum_i P_i + \sum_n V_n^s = \sum_n D_n \tag{2a}$$

$$-\bar{F}_l \le \sum_n \Gamma_{l,n} \Big(\sum_{i \in \mathcal{G}(n)} P_i + V_n^s - D_n \Big) \le \bar{F}_l, \forall l \in \mathcal{N}_l \tag{2b}$$

$$P_i^{\min} \le P_i \le P_i^{\max}, \forall i \in \mathcal{N}_g \tag{2c}$$

$$V_n^s \le V_n^f, \ \forall n \in \mathcal{N}_b, \tag{2d}$$

$$V_n^s - \underline{V}_n^f \le U_n^{\text{LB}}, \quad n \in \mathcal{N}_b, \tag{2e}$$

$$\underline{V}_n = V_n^s - U_n^{\text{LB}}, \ \bar{V}_n = V_n^s + U_n^{\text{UB}}, \quad n \in \mathcal{N}_b \tag{2f}$$

[2]It follows the current practice in industry. There are rich discussions on other objectives in literature, such as [28]. Among them is removing congestion revenue from social welfare [29]. On the contrary, some researchers believe congestion revenue should be counted as a part of the social surplus, as it is distributed to FTR holders [28]. Interested readers are referred to [28], [29] for detailed discussions.

$$\sum_i \hat{P}_i(\boldsymbol{v}) + \sum_n V_n = \sum_n D_n, \ \forall V_n \in [\underline{V}_n, \bar{V}_n] \tag{3a}$$

$$-\bar{F}_l \le \sum_n \Gamma_{l,n} \Big(\sum_{i \in \mathcal{G}(n)} \hat{P}_i(\boldsymbol{v}) + V_n - D_n \Big) \le \bar{F}_l, \quad \forall V_n \in [\underline{V}_n, \bar{V}_n], l \in \mathcal{N}_l \tag{3b}$$

$$R_i^{\text{down}} \delta \le \hat{P}_i(\boldsymbol{v}) - P_i \le R_i^{\text{up}} \delta, \forall V_n \in [\underline{V}_n, \bar{V}_n], i \in \mathcal{N}_g \tag{3c}$$

$$U_n^{\text{LB}}, U_n^{\text{UB}}, \underline{V}_n \ge 0, \forall n \in \mathcal{N}_b \tag{3d}$$

where P_i, D_n, V_n^s, U_n^{LB}, U_n^{UB}, $\underline{V}_n$, and $\bar{V}_n$ are decision variables at the first stage. P_i, D_n, $\underline{V}_n$, and $\bar{V}_n$ denote the output of Fully Controllable Generator (FCG) i, load at bus n, allowable lower and upper bound of VER injection at bus n, respectively. It is noted that the controllable load can also be modeled as FCG. As it is optimally determined and secure, $[\underline{V}_n, \bar{V}_n]$ is called Optimal Injection-Range (OIR). $\hat{P}_i(\boldsymbol{v})$ is the re-dispatch at the second stage when VER output $\boldsymbol{v}$ is revealed. Constant $\bar{F}_l$, $P_i^{\min}$, $P_i^{\max}$, R_i^{down}, R_i^{up}, and δ are, respectively, the transmission limit of line l, lower and upper bounds of generation of FCG i, downward and upward ramping rates, and timespan. Constant $\Gamma_{l,n}$ denotes the shift factor for line l and bus n. Like C_d being submitted by LSE, C_f can be submitted by the demander of flexibility, i.e., VER.

Equation (2a) denotes the power balance constraint; (2b) denotes the transmission line limit; (2c) represents the generation capacity. Equation (2e)-(2f) are the constraints for VER generators. They are well discussed at the beginning of this section. Equation (3a)-(3c) denote the constraints for the uncertainty accommodation at the second stage when the information on VER output is revealed. The ramping constraint (3c) is enforced for the re-dispatch of FCG.

III. Solution Approach

The co-optimization problem (1)-(3d) models infinite constraints for the re-dispatch process, which is sometimes called recourse in robust optimization literature [32]. The upward and downward flexibility, procured by VERs, are decision variables at the first stage. In this section, a general surrogate method is proposed to solve the problem of its kind.

For brevity, the model is first rewritten in a compact form

$$\text{(P)} \quad \min_{\boldsymbol{x},\boldsymbol{u}} \quad \boldsymbol{c}^\top \boldsymbol{x} - \boldsymbol{f}^\top \boldsymbol{u} \tag{4a}$$

$$\text{s.t.} \quad \boldsymbol{A}\boldsymbol{x} \le \boldsymbol{b} \tag{4b}$$

$$\boldsymbol{F}\boldsymbol{u} + \boldsymbol{H}\boldsymbol{x} \le \boldsymbol{h} \tag{4c}$$

$$\boldsymbol{B}\boldsymbol{x} + \boldsymbol{C}\boldsymbol{y}(\boldsymbol{\epsilon}) + \boldsymbol{E}\boldsymbol{\epsilon} \le \boldsymbol{d}, \forall \boldsymbol{\epsilon} \in \mathcal{U}(\boldsymbol{u}) \tag{4d}$$

where variable $\boldsymbol{x}$ includes the generation dispatch, VER's scheduled output, and the load. The variable $\boldsymbol{u}$ denotes the flexibility procured by VER. It includes the downward deviation bound $\boldsymbol{u}^{\text{LB}} \in \mathbb{R}^{N_b}$ and the upward deviation bound $\boldsymbol{u}^{\text{UB}} \in \mathbb{R}^{N_b}$, where N_b is the number of buses. Thus, the system must maintain enough flexibility at the first stage such that it can accommodate these deviations of VER outputs at the second stage. Equation (4a) denotes the objective function (1). It could be a linear or semi-positive quadratic function. Equation (4b) denotes (2a)-(2d). Equation (2e)-(2f) are represented by (4c). The re-dispatch constraints (3a)-(3c) are rewritten in (4d). The function $\boldsymbol{y}(\boldsymbol{\epsilon}) : \mathbb{R}^{N_b} \to \mathbb{R}^{N_g}$

is an image of uncertainty $\boldsymbol{\epsilon} \in \mathbb{R}^{N_b}$, where N_g and N_b are numbers of FCGs and VER generators, respectively. It represents the corrective actions (or re-dispatch) of FCGs when the uncertainty is revealed. The uncertainty is defined as

$$\epsilon_n = V_n - V_n^s,\ \forall n \in \mathcal{N}_b.$$

In other words, ϵ_n is a deviation of realized VER generation V_n from the scheduled one V_n^s. The uncertainty set is defined as

$$\mathcal{U}(\boldsymbol{u}) \triangleq \{\boldsymbol{\epsilon} \in \mathbb{R}^{N_b} : -\boldsymbol{u}^{\text{LB}} \leq \boldsymbol{\epsilon} \leq \boldsymbol{u}^{\text{UB}}\},$$

where $\boldsymbol{u}^{\text{LB}} \geq \mathbf{0}$ and $\boldsymbol{u}^{\text{UB}} \geq \mathbf{0}$.

A. Surrogate Affine Approximation

Problem (P) is computationally intractable due to the infinite constraints (4d). On the other hand, $\mathcal{U}(\boldsymbol{u})$ is a function of $\boldsymbol{u}$ and its extreme points are unknown. Hence, problem (P) cannot be solved directly by extreme point-based approaches, which are often used to handle infinite constraints in robust optimization literature [7], [32], [33]. The problem of DNE-limit search has a similar structure [23]. It was viewed as an intractable nonlinear problem. Hence, ISO-NE uses a heuristic method to set re-dispatch strategy, instead of finding the optimal one. Next, it is shown why the traditional affine policy is intractable to solve problem (P).

Consider the traditional affine policy

$$\boldsymbol{y}(\boldsymbol{\epsilon}) = \boldsymbol{G}\boldsymbol{\epsilon}, \tag{5}$$

where $\boldsymbol{G} \in \mathbb{R}^{N_g \times N_b}$ is the matrix of affine policy. It maps the uncertainty to re-dispatch. With the restricted recourse $\boldsymbol{G}\boldsymbol{\epsilon}$, the jth row of constraint (4d) becomes

$$0 \geq \begin{Bmatrix} \max\limits_{\boldsymbol{\epsilon}} & (\boldsymbol{C}\boldsymbol{G} + \boldsymbol{E})_j \boldsymbol{\epsilon} + \boldsymbol{B}_j \boldsymbol{x} - d_j \\ \text{s.t.} & -\boldsymbol{u}^{\text{LB}} \leq \boldsymbol{\epsilon} \leq \boldsymbol{u}^{\text{UB}} \end{Bmatrix}, \forall j \in \mathcal{J} \tag{6}$$

where $(\cdot)_j$ denotes the jth row of matrix/vector. It is noted that $\boldsymbol{u}^{\text{LB}}$ and $\boldsymbol{u}^{\text{UB}}$ are non-negative vectors. $\mathcal{J}$ is the set of rows in (4d). Equation (6) shows that value of

$$(\boldsymbol{C}\boldsymbol{G} + \boldsymbol{E})_j \boldsymbol{\epsilon} + \boldsymbol{B}_j \boldsymbol{x} - d_j$$

is never greater than zero for any $\boldsymbol{\epsilon}$ respecting

$$-\boldsymbol{u}^{\text{LB}} \leq \boldsymbol{\epsilon} \leq \boldsymbol{u}^{\text{UB}}.$$

In other words, when $\boldsymbol{\epsilon}$ is revealed, the corrective action $\boldsymbol{G}\boldsymbol{\epsilon}$ respects the system-wide constraints.

Following strong duality [34], equation (6) is exactly recast as

$$\begin{cases} \boldsymbol{C}\boldsymbol{G} + \boldsymbol{E} + \boldsymbol{\pi}^{\text{LB}} - \boldsymbol{\pi}^{\text{UB}} = \mathbf{0} & \text{(7a)} \\ \boldsymbol{B}\boldsymbol{x} - \boldsymbol{d} + \boldsymbol{\pi}^{\text{LB}}\boldsymbol{u}^{\text{LB}} + \boldsymbol{\pi}^{\text{UB}}\boldsymbol{u}^{\text{UB}} \leq \mathbf{0} & \text{(7b)} \\ \boldsymbol{\pi}^{\text{LB}}, \boldsymbol{\pi}^{\text{UB}} \geq \mathbf{0} & \text{(7c)} \end{cases}$$

where $\boldsymbol{x}$, $\boldsymbol{G}$, $\boldsymbol{\pi}^{\text{LB}}$, $\boldsymbol{\pi}^{\text{UB}}$, $\boldsymbol{u}^{\text{LB}}$ and $\boldsymbol{u}^{\text{UB}}$ are variables. Equation (6) is equivalent to (7a)-(7c), an approximation to the original constraint (4d). As a side note, affine policy is often employed in stochastic programming and robust optimization literature due to its computational tractability [9], [11], [26], [35]. However, equation (7b) is computationally intractable due to bilinear term $\boldsymbol{\pi}^{\text{LB}}\boldsymbol{u}^{\text{LB}}$ and $\boldsymbol{\pi}^{\text{UB}}\boldsymbol{u}^{\text{UB}}$ resulted from the traditional affine policy.

Next, a new SAA method is proposed to solve the problem in polynomial time. Fundamentally, the SAA method introduces new variables to replace bilinear term $\boldsymbol{\pi}^{\text{LB}}\boldsymbol{u}^{\text{LB}}$ and $\boldsymbol{\pi}^{\text{UB}}\boldsymbol{u}^{\text{UB}}$. The new constraints without nonlinear terms are surrogates to the original ones. The proposed technique does not relax any constraints, even better, it increases the freedom degree of affine policy. While techniques are different, the terminology "surrogate" can date back to 1990s in Lagrangian Relaxation literature [36]. Authors in [36] propose to update Lagrangian multipliers by solving only some rather than all subproblems.

To eliminate the bilinear terms in (7b), two surrogates are designed in the SAA method. The original uncertainty set $\mathcal{U}(\boldsymbol{u})$ is the underlying cause of nonlinearity. The proposed two surrogates are thus used to replace $\mathcal{U}(\boldsymbol{u})$. One is a surrogate uncertainty set, and the other is a surrogate function. Define the new surrogate uncertainty set

$$\tilde{\mathcal{U}} \triangleq \left\{(\boldsymbol{\delta}^{\text{LB}}, \boldsymbol{\delta}^{\text{UB}}) \in \mathbb{R}^{2N_b} : \mathbf{0} \leq \boldsymbol{\delta}^{\text{LB}} \leq \mathbf{1}, \mathbf{0} \leq \boldsymbol{\delta}^{\text{UB}} \leq \mathbf{1}\right\}. \tag{8}$$

The surrogate uncertainty set $\tilde{\mathcal{U}}$ is constant. Define the surrogate function $\boldsymbol{s}(\boldsymbol{u}^{\text{LB}}, \boldsymbol{u}^{\text{UB}}) : \mathbb{R}^{2N_b} \to \mathbb{R}^{2N_b}$

$$\boldsymbol{s}(\boldsymbol{u}^{\text{LB}}, \boldsymbol{u}^{\text{UB}}) \triangleq \text{diag}(\boldsymbol{u}^{\text{UB}})\boldsymbol{\delta}^{\text{UB}} - \text{diag}(\boldsymbol{u}^{\text{LB}})\boldsymbol{\delta}^{\text{LB}},$$

where $\text{diag}(\cdot)$ is a diagonal matrix whose diagonal entries are elements of vector $\cdot$. Then the image of $\tilde{\mathcal{U}}$ under the surrogate function $\boldsymbol{s}(\boldsymbol{u}^{\text{LB}}, \boldsymbol{u}^{\text{UB}})$ is

$$\hat{\mathcal{U}} \triangleq \left\{ \text{diag}(\boldsymbol{u}^{\text{UB}})\boldsymbol{\delta}^{\text{UB}} - \text{diag}(\boldsymbol{u}^{\text{LB}})\boldsymbol{\delta}^{\text{LB}} : (\boldsymbol{\delta}^{\text{LB}}, \boldsymbol{\delta}^{\text{UB}}) \in \tilde{\mathcal{U}} \right\}.$$

A lemma is established as follows regarding the primitive set and the image of the surrogate set.

Lemma 1. *The image of the uncertainty set $\tilde{\mathcal{U}}$ under the surrogate function $\boldsymbol{s}(\boldsymbol{u}^{LB}, \boldsymbol{u}^{UB})$ is equivalent to $\mathcal{U}$, i.e., $\mathcal{U}(\boldsymbol{u}) = \hat{\mathcal{U}}$.*

The proof is trivial. Lemma 1 reveals that any original uncertainty point in $\mathcal{U}$ can be replaced with its image in the surrogate set $\hat{\mathcal{U}}$. Based on Lemma 1, propositions are established as follows concerning the computational tractability.

Proposition 1. *Let $\boldsymbol{U}^{LB} = \text{diag}(\boldsymbol{u}^{LB})$ and $\boldsymbol{U}^{UB} = \text{diag}(\boldsymbol{u}^{UB})$. Then, constraint* (4d) *is rewritten as*

$$\boldsymbol{B}\boldsymbol{x} + \boldsymbol{C}\hat{\boldsymbol{y}}(\boldsymbol{\delta}^{LB}, \boldsymbol{\delta}^{UB}) + \boldsymbol{E}\begin{bmatrix} -\boldsymbol{U}^{LB} & \boldsymbol{U}^{UB} \end{bmatrix}\begin{bmatrix} \boldsymbol{\delta}^{LB} \\ \boldsymbol{\delta}^{UB} \end{bmatrix} \leq \boldsymbol{d}, \quad \forall (\boldsymbol{\delta}^{LB}, \boldsymbol{\delta}^{UB}) \in \tilde{\mathcal{U}}, \tag{9}$$

where $\hat{\boldsymbol{y}}(\boldsymbol{\delta}^{LB}, \boldsymbol{\delta}^{UB}) : \mathbb{R}^{2N_b} \to \mathbb{R}^{N_g}$ is the surrogate re-dispatch function of uncertainty $(\boldsymbol{\delta}^{LB}, \boldsymbol{\delta}^{UB})$.

According to the definition of $\hat{\mathcal{U}}$, $\begin{bmatrix} -\boldsymbol{U}^{\text{LB}} & \boldsymbol{U}^{\text{UB}} \end{bmatrix}\begin{bmatrix} \boldsymbol{\delta}^{\text{LB}} \\ \boldsymbol{\delta}^{\text{UB}} \end{bmatrix} \in \hat{\mathcal{U}}, \forall (\boldsymbol{\delta}^{\text{LB}}, \boldsymbol{\delta}^{\text{UB}}) \in \tilde{\mathcal{U}}$. Following Lemma 1, $(\boldsymbol{x}, \boldsymbol{u}^{\text{LB}}, \boldsymbol{u}^{\text{UB}})$ respecting (9) must be feasible for (6).

Proposition 2. *Consider a surrogate affine function*

$$\hat{\boldsymbol{y}}(\boldsymbol{\delta}^{LB}, \boldsymbol{\delta}^{UB}) = \hat{\boldsymbol{G}}\begin{bmatrix} \boldsymbol{\delta}^{LB} \\ \boldsymbol{\delta}^{UB} \end{bmatrix}. \tag{10}$$

Following the strong duality, the surrogate affine approximation of (4d) *is*

$$\begin{cases} \boldsymbol{C}\hat{\boldsymbol{G}} + \boldsymbol{E}\Big[-\boldsymbol{U}^{LB} \quad \boldsymbol{U}^{UB}\Big] - \boldsymbol{\pi} \le \boldsymbol{0} & \text{(11a)} \\ \boldsymbol{B}\boldsymbol{x} - \boldsymbol{d} + \boldsymbol{\pi}\cdot\boldsymbol{1} \le \boldsymbol{0} & \text{(11b)} \\ \boldsymbol{\pi} \ge \boldsymbol{0} & \text{(11c)} \end{cases}$$

where $\boldsymbol{x}, \hat{\boldsymbol{G}}, \boldsymbol{\pi}, \boldsymbol{u}^{LB}$ *and* $\boldsymbol{u}^{UB}$ *are variables.*

Compared to (7a)-(7b), equation (11a)-(11c) do not have any nonlinear terms. Bilinear term $\boldsymbol{\pi}^{\text{LB}}\boldsymbol{u}^{\text{LB}}$ and $\boldsymbol{\pi}^{\text{UB}}\boldsymbol{u}^{\text{UB}}$ in (7b) are replaced with linear term $\boldsymbol{\pi}\cdot\boldsymbol{1}$ in (11b). Equation (11a)-(11c) are linear and computationally tractable. Following Proposition 2, the SAA model

$$\begin{aligned} \text{(SAA-P)} \quad J_{\text{APP}} = \min_{\boldsymbol{x},\boldsymbol{u},\hat{\boldsymbol{G}}} \quad & \boldsymbol{c}^\top\boldsymbol{x} - \boldsymbol{f}^\top\boldsymbol{u} \\ \text{s.t.} \quad & \text{(4b)} - \text{(4c)}, \text{(11a)} - \text{(11c)} \end{aligned}$$

is formulated, and it can be solved using modern LP solvers. In problem (SAA-P), the decision variables are generation dispatch, VER's scheduled output, load demand, upward/downward flexibility, and surrogate affine policy.

Surrogate affine policy $\hat{\boldsymbol{G}}$ in problem (SAA-P) is used for re-dispatch once the uncertainty is revealed. After optimal $\hat{\boldsymbol{G}}$ is attained, the re-dispatch can be written as

$$\hat{\boldsymbol{G}}\begin{bmatrix}\boldsymbol{\delta}^{\text{LB}} \\ \boldsymbol{\delta}^{\text{UB}}\end{bmatrix} = \hat{\boldsymbol{G}}\begin{bmatrix}\max\left(-(\boldsymbol{U}^{\text{LB}})^{-1}\boldsymbol{\epsilon}, \boldsymbol{0}\right) \\ \max\left(-(\boldsymbol{U}^{\text{UB}})^{-1}\boldsymbol{\epsilon}, \boldsymbol{0}\right)\end{bmatrix} \quad (12)$$

$$= \hat{\boldsymbol{G}}\begin{bmatrix}(\boldsymbol{U}^{\text{LB}})^{-1} & \boldsymbol{0} \\ \boldsymbol{0} & (\boldsymbol{U}^{\text{UB}})^{-1}\end{bmatrix}\begin{bmatrix}\max\left(-\boldsymbol{\epsilon}, \boldsymbol{0}\right) \\ \max\left(\boldsymbol{\epsilon}, \boldsymbol{0}\right)\end{bmatrix}. \quad (13)$$

Above two equality equations naturally introduce two ways to calculate re-dispatch when uncertainty $\boldsymbol{\epsilon}$ is realized. Equation (12) shows one way that requires the calculation of the surrogate uncertainty. In contrast, (13) shows the other way without such calculation. One can calculate

$$\hat{\boldsymbol{G}}\begin{bmatrix}(\boldsymbol{U}^{\text{LB}})^{-1} & \boldsymbol{0} \\ \boldsymbol{0} & (\boldsymbol{U}^{\text{UB}})^{-1}\end{bmatrix}$$

without uncertainty $\boldsymbol{\epsilon}$ information in advance. It is preprocessing of the surrogate affine policy.

B. Optimality of SAA

In Section III-A, the SAA method is introduced to solve the co-optimization model. In this part, its optimality is analyzed by being compared with that of the conventional affine policy.

Proposition 3. *Denote the feasible region of* $(\boldsymbol{x}, \boldsymbol{u})$ *in (SAA-P) as* $\mathcal{F}_{saa}$*. Consider the traditional affine policy model*

$$\begin{aligned} \textit{(TAP-P)} \quad J_{AP} = \min_{\boldsymbol{x},\boldsymbol{u},\boldsymbol{G}} \quad & \boldsymbol{c}^\top\boldsymbol{x} - \boldsymbol{f}^\top\boldsymbol{u} \\ \textit{s.t.} \quad & \text{(4b)} - \text{(4c)}, \text{(7a)} - \text{(7c)}, \end{aligned}$$

and denote the feasible region of $(\boldsymbol{x}, \boldsymbol{u})$ *in (TAP-P) as* $\mathcal{F}_{tap}$*, then* $\mathcal{F}_{tap} \subseteq \mathcal{F}_{saa}$ *always holds.*

Proof. Assume global optimal solution $(\boldsymbol{x}^*, \boldsymbol{u}^*, \boldsymbol{G}^*)$ to intractable problem (TAP-P) is attained from an oracle. The surrogate affine policy is constructed as

$$\hat{\boldsymbol{G}}^* = [-\boldsymbol{G}^*\boldsymbol{U}^{\text{LB}} \quad \boldsymbol{G}^*\boldsymbol{U}^{\text{UB}}].$$

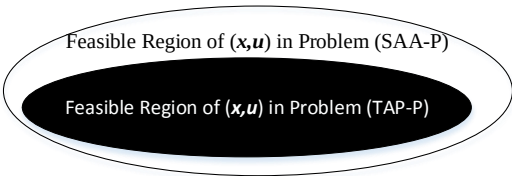

Fig. 2. Comparison of feasible regions of the conventional affine policy and the surrogate affine policy-based approaches.

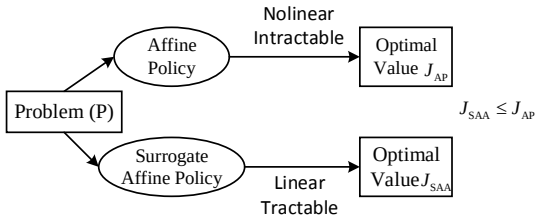

Fig. 3. Comparison of conventional affine policy and surrogate affine policy.

Given any uncertainty $\boldsymbol{\epsilon} \in [-\boldsymbol{u}^{\text{LB}}, \boldsymbol{u}^{\text{UB}}]$, a surrogate uncertainty can be constructed as

$$\boldsymbol{\delta}^{\text{LB}} = \max\left(-(\boldsymbol{U}^{\text{LB}})^{-1}\boldsymbol{\epsilon}, \boldsymbol{0}\right), \boldsymbol{\delta}^{\text{UB}} = \max\left((\boldsymbol{U}^{\text{UB}})^{-1}\boldsymbol{\epsilon}, \boldsymbol{0}\right),$$

where $\max(\cdot,\cdot)$ returns a component-wise maximum vector. $(\boldsymbol{x}^*, \boldsymbol{u}^*, \hat{\boldsymbol{G}}^*)$ is a feasible point to problem (SAA-P). Therefore, $\mathcal{F}_{\text{tap}} \subseteq \mathcal{F}_{\text{saa}}$. □

Proposition 3 indicates that the feasible region of $(\boldsymbol{x}, \boldsymbol{u})$ in SAA-based model is never smaller than that in the conventional affine policy-based model. Due to the higher freedom degree of the surrogate affine policy, it is possible that the feasible region of the conventional affine policy-based model is a strict subset of that of the SAA-based model. This case is illustrated in Fig. 2. The following lemma shows the relation between the optimal values obtained using these two methods.

Lemma 2. *If problem (SAA-P) and (TAP-P) are feasible, then*

$$J_{SAA} \le J_{AP}$$

holds, where J_{SAA} *and* J_{AP} *denote the optimal values of problem (SAA-P) and (TAP-P), respectively.*

The proof is trivial given Proposition 3. If $\mathcal{F}_{\text{tap}} \subset \mathcal{F}_{\text{saa}}$ holds, then $J_{\text{SAA}} < J_{\text{AP}}$ holds sometimes. It is shown in [37] that separating the uncertainty into upward and downward parts can improve the solution. Fig. 3 illustrates a comparison between two methods. In the SAA method, one only needs to handle tractable linear constraints. In contrast, one has to deal with an intractable nonlinear problem in the conventional affine policy-based method.

C. Extension to Multi-period ED

The co-optimization model and solution approach is readily extended to the multi-period ED. Consider period index $t = \{1, \cdots, T\}$. The objective function (1) and constraint (2a)-(3c) are repeated over all periods. The generation output is subject to ramping up/down constraints

$$R_i^{\text{down}}\delta \le P_{i,t} - P_{i,t+1} \le R_i^{\text{up}}\delta, \quad \forall i \in \mathcal{I},\ t = 1, \cdots, T-1.$$

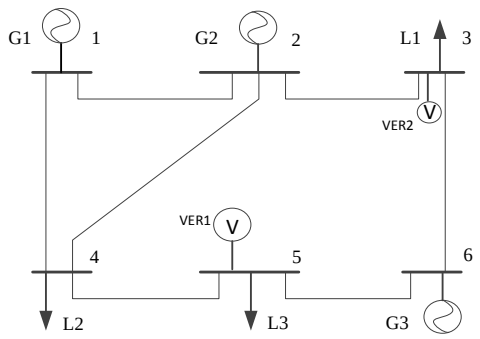

Fig. 4. The one-line diagram for the six-bus system

Constraints between $\hat{P}_{i,t}$ and $\hat{P}_{i,t+1}$ can also be enforced. Equation (4d) is general enough to include these ramping constraints, and the proposed solution approach is still applicable. It is noted ISO/RTO runs ED tool on a rolling basis, and only issues dispatch signal for the first interval in practice.

To simplify the policy, $\boldsymbol{G}$ can be restricted to depend only on the most recently revealed information $\boldsymbol{v}_t$. A multi-stage model is thus attained since the re-dispatch decision at t can be made based on all available information at time t. In the proposed SAA method, the resulting problem (SAA-P) is convex and has a similar structure with the conventional affine policy-based multi-stage model [38].

D. Application in DNE-limit Search

The proposed SAA method can also be directly applied to the problem of DNE-limit search in ISO-NE. The DNE-limit search is the sequential optimization, where the regular ED problem is first solved, and then a problem maximizing the DNE-limit is formulated given the ED solution. It has several advantages to apply the SAA method in the DNE-limit search. Firstly, the SAA method gets optimal participation factors in polynomial time. Secondly, SAA provides an adjustment matrix with higher freedom degree for the controllable generators. More specifically, the optimal participation factors for upward uncertainties can be different from those for downward uncertainties. Thirdly, due to tractability of SAA, one can solve two problems sequentially to get a larger injection-range when a multiplicity of ED occurs. The first one is a regular ED problem, whose optimal value will be enforced as a constraint in the second problem, i.e., DNE-limit search. Alternatively, one can also get the ED and DNE-limit in one shot by solving problem (SAA-P) with a special $\boldsymbol{f}$ that has small elements. These advantages in return help integrate more VERs.

IV. Case Studies

The simulations were performed in a six-bus system and a modified IEEE 118-bus system to illustrate the proposed model and SAA method. All cases were solved using CPLEX 12.7 on a PC with 2.6 GHz Intel Core i7.

A. Six-bus system

Fig. 4 shows the one-line diagram of the six-bus system. There are three FCGs, two VER units, and three loads.

TABLE I
FULLY CONTROLLABLE GENERATORS IN SIX-BUS SYSTEM

	$P^{\min}$*	$P^{\max}$*	$R^{\text{down}}/R^{\text{up}}$***	S1-IC**	S2-IC **	S3-IC **
G1	100	210	12	10	10	10
G2	10	100	6	10	13	13
G3	0	20	5	10	10	18

* MW; ** incremental cost, \$/MWh; *** MW/Interval

TABLE II
COMPARISON OF FINDING OPTIMAL FLEXIBILITY IN THREE CASES IN THE SIX-BUS SYSTEM

	Decision Variable	Parameter
Case 1 (sequential opt.)	up./down. flexibility	$\boldsymbol{G}$, ED
Case 2 (sequential opt.)	up./down. flexibility, $\boldsymbol{G}$	ED
Case 3 (Co-opt.)	up./down. flexibility, $\boldsymbol{G}$, ED	

Table I shows parameters of three FCGs. All generators are committed. For simplicity, only a single-period scheduling problem was considered. Three scenarios, S1, S2, and S3, were considered with different Incremental Costs (ICs) for FCG. Forecast outputs of VER1 and VER2 are 16 MW and 10 MW, respectively. The upward deviations are 16 MW and 14 MW; the downward deviations are 15 MW and 8 MW, respectively. The following case studies were performed in the six-bus system:

- Case 1: Sequential optimization with fixed AP.
- Case 2: Sequential optimization with variable AP.
- Case 3: Co-optimization with variable AP.

In the six-bus system, flexibility is held for the deviation of VER output. Hence, it is gauged by allowable injection-range for VERs. Table II shows the main differences in three cases. In Case 1, flexibility/injection-range for VER was calculated given $\boldsymbol{G}$ and ED solution. In Case 2, the injection-range and $\boldsymbol{G}$ are decision variables given ED solution. As the search of maximum injection-range for VERs finishes in two steps, it is the so-called sequential optimization in Case 1 and 2. In Case 3, injection-range, ED solution, and $\boldsymbol{G}$ were optimized simultaneously. The transmission constraints were relaxed in Case 1 and 2, so that it is easy to illustrate the basic ideas. For comparison, the transmission constraints were enforced in Case 3.

1) Case 1: In this case, there are two steps to determine the injection-range for VER or flexibility. The first step is to solve a classic ED model that determines the FCG power outputs. The second step is to find the maximal secure injection-range for VER, given the ED solution to the first problem. In Case 1, the constraint (2e) was dropped. This case is similar to the DNE limit search in ISO-NE [23].

Table III shows the ED solutions in three scenarios with different ICs. It is observed that the total cost rises with increasing ICs. The lowest cost is \$2684 in the scenario with ICs, \$10/MWh, for G1, G2, and G3. The scheduled VER outputs are 16 MW and 10 MW, respectively. They reach the limits (i.e., forecast values) according to constraint (2d), as VER generators' IC, \$0/MWh, is much cheaper than other generators' IC, \$10/MWh.

In this case, the affine adjustment matrix is

TABLE III
GIVEN ECONOMIC DISPATCHES FOR SEQUENTIAL OPTIMIZATION WITH DIFFERENT INCREMENTAL COSTS IN CASE 1 AND 2

	G1(MW)	G2(MW)	G3(MW)	VER1(MW)	VER2(MW)	Cost ($)
S1	204	15	5	16	10	2684
S2	205	10	9	16	10	2714
S3	210	14	0	16	10	2726

TABLE IV
FLEXIBILITY FOR VERS (MW)

	Up.VER1	Up.VER2	Dn.VER1	Dn.VER2
S1	10	1.5	10	1.5
S2	0	0	0	0
S3	0	0	0	0

$$-\begin{bmatrix} 0.5217 & 0.5217 \\ 0.26087 & 0.26087 \\ 0.2174 & 0.2174 \end{bmatrix}, \tag{14}$$

which was determined proportionally according to the ramping rate of FCG. Although it is non-optimal, a similar strategy is used in industry, as finding the optimal adjustment matrix was regarded as computationally intractable in the traditional affine policy-based method. As a side note, the SAA method can find the optimal adjustment matrix in polynomial time. Based on the ED solution and the adjustment matrix (14), it is trivial to calculate corrected dispatches and injection-ranges for VER. For instance, if the realized VER outputs are 17 MW and 12 MW, respectively, the adjusted output vector in S1 is

$$\begin{bmatrix} 202.9565 \\ 14.4783 \\ 4.5652 \end{bmatrix} = \begin{bmatrix} 204 \\ 15 \\ 5 \end{bmatrix} - \begin{bmatrix} 0.5217 & 0.5217 \\ 0.26087 & 0.26087 \\ 0.2174 & 0.2174 \end{bmatrix} \begin{bmatrix} 17-16 \\ 12-10 \end{bmatrix}.$$

The allowed deviation ranges for the VER are shown in Table IV. It is observed that the system-wide upward deviation range is 11.5 MW (i.e., $11.5 = 10 + 1.5$) in S1. Column "Up. VER1" ("Dn.Ver1") is the upward (downward) deviation range for VER1. However, while G2 reaches its lower bound (i.e., 10 MW) in S2, and G3 reaches its lower bound (i.e., 0 MW) in S3, the deviation ranges are 0 MW in both S2 and S3, given the ED solution and the adjustment matrix (14).

2) Case 2: Similar to Case 1, the ED problem and injection-range search problem were solved sequentially, but with variable affine adjustment in this case. Given the ED solution, the proposed SAA method was used to find the secure injection-range. Table VI shows the secure injection-ranges for VER in Case 2. It is observed that the system-wide injection-range (or flexibility) is larger than that in Case 2. Next, detailed discussions and analysis of this advantage will be presented. Some limitations of sequential optimization, such as limitation of injection-range and infeasibility, will be discussed.

First, the larger injection-range partially comes from the optimality of the affine adjustment. Case 2 has the same ED solution with Case 1, as both employ the same ED model. In contrast, the adjustment matrix is a decision variable in Case 2. In the problem of optimizing injection-range/deviation range/flexibility, the same coefficient for VER1 and VER2 were used. In the SAA method, one can attain the optimal solution by solving an LP problem. Table V presents the optimal surrogate affine adjustment matrices in scenario S1, S2, and S3, and Table VI presents the largest allowed deviations for VER in different scenarios. Table V shows three 3×4 matrices. The re-dispatch can be calculated based on (12)-(13) according to Table V and VI. For example, consider realized VER1 and VER2 output being 10 MW and 13 MW, respectively. Then, the output vector after re-dispatch in S1 is

$$\begin{bmatrix} 203.5462 \\ 17.1176 \\ 6.3361 \end{bmatrix} = \begin{bmatrix} 204 \\ 15 \\ 5 \end{bmatrix} + \begin{bmatrix} 0 & -12 & 6 & 0 \\ -5 & 0 & 6 & 0 \\ -3 & -2 & 5 & 0 \end{bmatrix} \begin{bmatrix} \max\{0, \frac{10-16}{17}\} \\ \max\{0, \frac{13-10}{17}\} \\ \max\{0, \frac{16-10}{14}\} \\ \max\{0, \frac{10-13}{14}\} \end{bmatrix},$$

where $(16-10)/17$ and $(13-10)/14$ are the surrogate uncertainties from VER1 and VER2, respectively. By comparing the data in Table IV and VI, one can find that the deviation range is larger in Case 2, even Case 1 and 2 have the same ED. For example, in scenario S1, the total upward deviation range increases to 22 MW (i.e., $22 = 8 + 14$) from 11.5 MW. At the same time, the downward deviation range also increases to 17 MW from 11.5 MW, although up to 16 MW is useful.

TABLE V
OPTIMAL SURROGATE AFFINE ADJUSTMENT MATRICES IN CASE 2 (MW)

	S1*				S2*				S3*			
	δ_1^{UB}	δ_2^{UB}	δ_1^{LB}	δ_2^{LB}	δ_1^{UB}	δ_2^{UB}	δ_1^{LB}	δ_2^{LB}	δ_1^{UB}	δ_2^{UB}	δ_1^{LB}	δ_2^{LB}
G1	0	-12	6	0	0	-12	0	5	0	-12	0	0
G2	-5	0	6	0	0	0	6	0	-4	0	0	6
G3	-3	-2	5	0	-3	-2	0	5	0	0	0	5

* 3×4 matrix.

TABLE VI
OPTIMAL ALLOWED DEVIATION RANGE FOR VER IN CASE 2 (MW)

	Up.VER1	Up.VER2	Dn.VER1	Dn.VER2
S1	8	14	17	0
S2	3	14	6	10
S3	4	12	0	11

Second, the larger injection-range for VER is partly because of the higher dimension of affine policy in SAA method. As each uncertainty was separated into virtual positive and negative components, various affine coefficients can be utilized for re-dispatch when uncertainties fall into different regions. In Case 1, the affine adjustment matrix is in the space of $\mathbb{R}^{3\times2}$. In contrast, the affine adjustment matrix is in the space of $\mathbb{R}^{3\times4}$ in Case 2. Take scenario S2 as an example. As G2's output is at its lower bound 10 MW, it cannot further lower its output. Therefore, G2 is not able to provide the downward flexible resource. In Case 1, although G2 has the ability to provide the upward reserves, the adjustment coefficients are all zeros limited by its zero downward reserves. In contrast, G2's coefficient of surrogate uncertainty (negative component) for VER1 is 6, according to column "δ_1^{LB}" for scenario S2 and row "G2" in Table V. At the same time, the allowed downward deviation for VER1 is 6 MW, and the corresponding surrogate uncertainty is $1 = 6/6$. It means that all the upward reserve of G2 will be utilized for the uncertainty management according to equation (10) (i.e., $6 = 6 \times \frac{6}{6}$). Consequently, the system has more flexibility to accommodate VER output in Case 2.

However, although the SAA method helps get the optimal secure injection-range, the largest possible injection-range for

TABLE VII
EDS FROM THE CO-OPTIMIZATION WITHOUT TRANSMISSION CONSTRAINTS IN CASE 3

	G1(MW)	G2(MW)	G3(MW)	VER1(MW)	VER2(MW)	Cost ($)
S1	198	21	5	16	10	2684
S2	198	11	15	16	10	2717
S3	198	26	0	16	10	2762

TABLE VIII
OPTIMAL ALLOWED DEVIATIONS OF VER GENERATION WITHOUT TRANSMISSION CONSTRAINTS IN CASE 3

	Up1	Up2	Dn1	Dn2	Δ Up [a]	Δ Dn [b]
S1	9	14	15	8	1	6
S2	9	14	15	8	6	7
S3	4	14	15	8	2	12

[a] Change of allowed upward deviations of VER generation from Case 2.
[b] Change of allowed downward deviations of VER generation from Case 2.

VER is still constrained by the available flexible resources. These flexible resources are determined as byproducts of solving the ED problem. According to Table VI, different EDs lead to various injection-ranges. For example, the total downward deviation in scenario S1 is 17 MW, which is larger than that of 11 MW in scenario S3. One can observe similar trends for the total upward deviations in different scenarios.

The simulation results also show that the secure injection-range obtained from the sequential optimizations may be infeasible in reality. The infeasibility is due to the fact that the VER generator can only spill power, but not produce electricity larger than its maximum available power. When the available VER power is smaller than the lower bound of the secure injection-range, it is impossible to enforce the lower bound limit for VER generator. For example, the allowed downward deviation range is 11 MW in scenario S3 according to Table VI. It indicates power produced by VERs should be at least 15 MW (i.e., $15 = 16 + 10 - 11$). However, there is a possibility that the available VER power is 3 MW (i.e., $3 = 16 - 15 + 10 - 8$). In this case, the secure downward range is infeasible. The similar defect exists in the DNE limit proposed by ISO-NE [23].

3) Case 3: In this case, the SAA method was employed to co-optimize the transactive flexibility, uncertainty, and energy. By solving one LP problem, one can get OIRs for VER, as well as the optimal power output of FCG (i.e., ED). The following context will illustrate how the proposed co-optimization model addresses the issues revealed in sequential optimization models. The results will verify its benefits in the social welfare and the VER injection-range.

For comparison purposes, the co-optimization model was formulated without transmission line constraints first, but with the feasibility constraint (2d). According to Table VII, the cost in scenario S1 remains $2684, and VERs are scheduled to generate power at the forecast values in Case 3. However, according to Table VII and Table VI, the total upward deviation for VERs increases by 1 MW (i.e., $1 = 9 + 14 - 8 - 14$) in scenario S1 from Case 2 to Case 3. Similarly, the downward deviation for VERs rises by 6 MW (i.e., $6 = 15+8-17-0$) in scenario S1. It suggests that the co-optimization model helps accommodate more VER power even though the total cost is the same. That is because ED problem, as an LP problem, often has multiple optimal solutions.

TABLE IX
ALLOWED UPWARD DEVIATION OF VERS WITH DIFFERENT FLEXIBILITY BIDS IN SCENARIO S3 IN CASE 3 WITHOUT TRANSMISSION CONSTRAINTS

VER1	VER2	Up-1	Up-2	G1	G2	G3	Cost ($)
4	4	16	2	198	26	0	2690
4	5.1	4	14	198	26	0	2674
4	6	4	14	198	26	0	2662
5.1	4	16	2	198	26	0	2673
5.1	6	9	14	198	21	5	2657
6	5.1	16	7	198	21	5	2655

Co-optimization also addresses the infeasibility issue in the sequential optimizations. Feasibility of VER injection-range comes at the expense of slightly higher total cost when bidding of flexibility is zero. For example, the total cost in scenario S3 is increased by $\$36 = \$2762 - \$2726$ from Case 2 to Case 3, according to Table III and VII. In Case 3, the VER generators can inject power within the range of $[3\text{ MW}, 44\text{ MW}]$ (i.e., $3 = 16 + 10 - 15 - 8, 44 = 16 + 10 + 4 + 14$) as shown in Table VII and VIII. In contrast, the range is $[15\text{ MW}, 42\text{ MW}]$ (i.e., $15 = 16 + 10 - 10, 40 = 16 + 10 + 4 + 12$) according to Table III and VI. More importantly, $[3\text{ MW}, 44\text{ MW}]$ is a feasible range. Therefore, the operator can guarantee that any VER power within the OIR will be securely accommodated.

An important question then arises: is it possible to further increase the secure injection-range of VERs (flexibility) or lower the total cost? Next, this question will be answered, and several interesting observations will be highlighted for the model with flexibility bids.

Firstly, the social welfare increases when VER generators are allowed to bid for flexibility. In Table IX, allowed upward deviations, column "Up-1" for VER1 and "Up-2" for VER2, are different with various flexibility bids in scenario S3. The bids are shown in column "VER1" and "VER2" in Table IX. The column 'Cost' in Table IX shows the total cost. For example, according to the 2nd row in Table IX, if the flexibility bids of VER1 and VER2, respectively, are \$4/MW and \$5.1/MW, then the allowed upward deviations for VER1 and VER2 are 4 MW and 14 MW, respectively. Compared to data in the 3rd row in Table VII, the total social welfare is increased by $\$72 = \$2762 - \$2690$ in Case 3, where the flexibility bids are introduced.

Secondly, the secure injection-range for VERs can be expanded when the bid reaches a certain level. For example, in the last two rows of Table IX where biddings are greater than \$5/MW, the system-wide allowed upward deviation increases to 23 MW (i.e., $23 = 9 + 14 = 16 + 7$) from 18 MW. In fact, 23 MW is the highest possible upward deviation (i.e., $23 = 12 + 6 + 5$). By comparing column "G3" in Table VII and Table III, one can observe that the increase of flexibility is due to the higher output of G3 in Case 3. If the upward deviation occurs, the system operator can lower G3's output to 0 MW so that G3 provides the additional 5 MW downward reserve. However, only when the flexibility bid is larger than

TABLE X
EDs AND ALLOWED UPWARD DEVIATIONS FOR VERs WITH FLEXIBILITY BIDS IN SCENARIO 3 WITH TRANSMISSION CONSTRAINTS

VER1	VER2	Up1	Up2	G1	G2	G3	Cost
4	4	4	14	148.14	75.86	0	2839.75
4	5.1	4	14	148.14	75.86	0	2824.37
4	6	4	14	148.14	75.86	0	2811.77
5.1	4	16	2	148.14	75.86	0	2822.17
5.1	6	9	14	148.88	70.12	5	2804.64
6	5.1	16	7	148.88	70.12	5	2802.84

TABLE XI
EDs AND ALLOWED UPWARD DEVIATIONS FOR VERs WITH FLEXIBILITY BIDS IN SCENARIO 3 WITH TRANSMISSION CONSTRAINTS

VER1	VER2	Up1	Up2	G1	G2	G3	Cost
4	4	12	6	168.0369	55.9631	0	2780.066
4	5.1	4	14	168.0369	55.9631	0	2764.666
4	6	4	14	168.0369	55.9631	0	2752.066
5.1	4	12	6	168.0369	55.9631	0	2766.866
5.1	6	9	14	168.7798	50.2202	5	2744.938
6	5.1	12	11	168.7798	50.2202	5	2746.738
11	5.1	16	7	164.7365	54.2635	5	2675.267

$5/MW (i.e., $5 = 18 - 13$), G3 will increase its output, and G2 will reduce its output. It verifies that introducing bid can help the system hold more flexibility.

Thirdly, VER1 and VER2 compete for the upward flexibility. By comparing the bids and the allowed upward deviations in Table IX, one can observe an interesting point that the VER generator with larger bid always has the larger allowed deviation. For example, when the bids from VER1 and VER2 are $4/MW and $6/MW, respectively, the procured upward flexibility by VER2 is 14 MW, which is 10 MW (i.e., $10 = 14 - 4$) higher than that of VER1. 14 MW is also the highest possible deviation of VER2. It suggests the co-optimization encourages VERs to bid for flexibility based on the benefit. From the system's perspective, flexibility will be positioned cost-effectively.

Now, consider the impacts of transmission line constraints. Table X presents the simulation results with enforced transmission line constraints. By comparing EDs in Table X and IX, one can observe that G1 produces less electricity. In contrast, G2 generates more electricity. That is due to the congestion of line 1-4. Moreover, the total cost increases when the transmission line constraint is enforced. For example, when bids are $4/MW from both VER generators, G1's scheduled output decreases by 49.86 MW (i.e., $49.86 = 198 - 148.14$), and G2's output increases by 49.86 MW (i.e. $49.86 = 75.86 - 26$). The total cost is $2839.75, which is increased by $149.75 (i.e., $149.75 = 2839.75 - 2690$). The allowed upward deviation does not change when the transmission line constraints are enforced in this case.

To analyze the impact on flexibility/OIR for VERs, VER1 was moved from bus 5 to bus 1. The results are shown in Table XI. By comparing the column 'G1', 'G2', and 'G3' in Table XI and X, one can observe that G1's output increases and G2's output decreases if VER is moved to bus 1. It is observed that when flexibility bids from VER1 and VER2 are $6/MW and $5.1/MW, respectively, the allowed deviation of VER1 is decreased to 12 MW from 16 MW according to Table XI and X, although system-wide flexibility remains 23 MW. If VER1 increases its bid to $11/MW, then the allowed deviation of VER1 decreases back to 16 MW. At the same time, the output of G1 decreases to 164.74 MW from 168.78 MW. It suggests that the congestion of line 1-3 prevents the larger power injection at bus 1. From the system's point of view, the benefit of providing upward flexibility at bus 1 is larger than that of using the cheap energy from G1, (i.e., $11 - 5.1 = 5.9 > 3 = 13 - 10$). Therefore, the upward flexibility is re-distributed between VER1 and VER2, and G2 supplies more loads in this case.

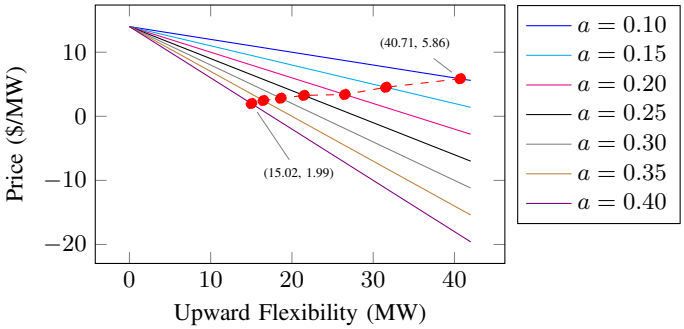

Fig. 5. Upward flexibility U^{UB} procured by VER27 when the load is 3060 MW. Solid lines denote bidding strategies ($2aU^{\text{UB}} + b$), which change with the increasing a. Red dots denote the optimal solutions with the increasing a.

B. Modified 118-bus System

The modified IEEE 118-bus system consists of 54 generators, 186 lines, and 91 loads. The VER generators are located at 18 buses. The detailed data for the model can be found at http://PowerEE.github.io/118_bus_data.xlsx. The sensitivity analysis was performed with various upward and downward flexibility bids. The simulation for the multi-period model was also performed. The quadratic curves were employed to simulate the flexibility benefit. For instance, the benefit of upward flexibility was assumed as $a_n(U_n^{\text{UB}})^2 + b_n(U_n^{\text{UB}}) + c_n$, where a_n, b_n and c_n are coefficients. The incremental benefit is $2a_nU_n^{\text{UB}} + b_n$. By changing a, one can easily modify benefit curves. Two scenarios were considered. Unit ON/OFF stats were assumed determined in advance.

In the first scenario, the load is 3030 MW. As the load is low, only a small number of units are committed. Figure 5 illustrates a set of the bidding curves with different a. For simplicity, it was assumed that all VER units use the same a, and the bids for the downward flexibility were set to 0 for all VER units. Generator VER27 is located at bus 27. It is observed that VER can procure more flexibility if its bid price is high. For example, if $a = 0.10$, then the bid of VER27 is $0.2U^{\text{UB}}+14$. In this case, the red dot $(40.71, 5.86)$ is the optimal point, which represents that VER27 can purchase 40.71 MW flexibility at the price of $5.86/MW. Alternatively, setting a to 0.40 indicates that VER27 willingness-to-pay is lower for upward flexibility. In this case, the optimal point is (15.02, 1.99), which means that VER27 purchases 15.02 MW

TABLE XII
PROCURED FLEXIBILITY WITH VARIOUS BIDS (LOAD: 3060 MW)

a***	Cost**	Scheduled*	Up. Flex.*	Down. Flex.*	OIR*
0.1	23302.93	1052.85	374.25	374.25	748.5
0.15	23745.04	1052.85	329.25	374.25	703.5
0.2	24066.74	1052.85	297.97	374.25	672.22
0.25	24290.77	1052.85	243.24	374.25	617.49
0.3	24446.95	1052.85	215.9	374.25	590.15
0.35	24572.91	1052.85	194.25	374.25	568.5
0.4	24682.09	1052.85	180.68	374.25	554.93

*** $/MW^2 ** $ * MW

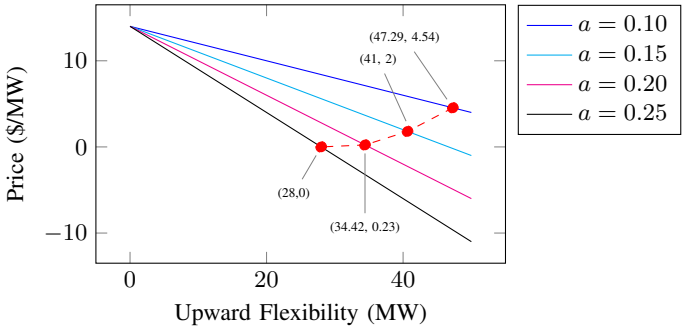

Fig. 6. Upward flexibility U^{UB} procured by VER27 when the load is 6060 MW. Solid lines denote bidding strategies ($2aU^{\text{UB}}+b$) that change with the increasing a. Red dots denote the optimal solutions with the increasing a.

flexibility at the price of $1.99/MW. The energy price at this location is around $12/MWh. The simulation results indicate that VERs can inject more clean energy into the grid by purchasing flexibility at a low price.

Table XII shows the system-wide information with increasing a. Column "Up. Flex." denotes system-wide upward flexibility. For example, $a = 0.1$ indicates that VER generators prefer to purchase more upward flexibility. The total cost is $23302.93, and upward flexibility is 374.25 MW, and system-wide OIR is 748.5 MW. Data in Table XII indicates that system-wide upward flexibility and the total cost (social welfare) are monotonically decreasing (increasing) with a. If a increases to 0.4 from 0.1, upward flexibility decreases by 193.57 MW (i.e., $193.57 = 374.25 - 180.68$) to 180.68 MW. As a result, OIR is reduced to 554.93 MW.

In the second scenario, the load was increased to 6060 MW, and more units were committed online (UC was determined in advance). Figure 6 shows the procured flexibility by VER27 with increasing a. It depicts a similar trend as Figure 5. If VER27 is willing to pay more, then it can procure more upward flexibility. An interesting observation is that VER27 can get 28 MW flexibility free of charge. It indicates that flexible resources are free products in some circumstances. At the same time, VER27 can also procure 40.65 MW flexibility at $1.8/MW, which is $4.06/MW (i.e., $4.06 = 5.86 - 1.8$) cheaper than that in the first scenario. It reveals that more flexibility will be available when more units are on-line.

An important trend is revealed that procured flexibility is a monotonically decreasing function of a in general. It indicates that the more VERs are willing to pay, the higher flexibility they can secure. Consequently, VERs can inject more energy into the grid. On the other hand, the total social welfare increases.

The model can be extended to the multi-period ED problem. ISOs/RTOs often perform multi-period ED problems on a rolling basis. To reduce the computational burden, the adjustment matrix was set to a diagonal block matrix. In return, the corrective actions of the FCGs are determined by the VER output deviation at the current interval. For a 24-period problem, LP solver was able to get the solution within 281 seconds. If inactive line constraints were removed based on [39], the solution time was reduced to 18 seconds, which is 6.4% of the original time.

V. CONCLUSION

With the growing VERs penetration, it becomes important to manage the demand of flexibility in the modern electric grid. This work provides an option to address these questions: 1) how to determine the flexibility amount while keeping ISO/RTO independent; 2) how to allocate flexibility to demander cost-effectively; 3) how to handle the high flexibility demand when the flexible resource is deficient. A model is proposed to optimize transactive flexibility, uncertainty, as well as energy. In this work, flexibility is defined as the change range of power injection that the system can accommodate using available flexible resources within a specified time.

A novel SAA method is proposed to solve the problem in polynomial time. It is proved that its solution is even better than the original affine policy-based method used in the power literature. The SAA method can also be applied to the DNE-limit search in the industry. The simulation results show the co-optimization approach increases the social welfare and proactively positions flexibility for VER accommodation.

As constraints in the SAA method are linear and convex, the general acceleration techniques for an LP/QP problem can be used directly in the proposed approach. By introducing decision variables and constraints associated with UC [3], [22], one can extend the co-optimization model to the UC problems. It will be an interesting future work, as UC may position more flexible resources.

The proposed model is convex, and Slater's condition holds. Thus, the strong duality follows. Therefore, it is possible to derive marginal prices for energy and upward/downward flexibility based on Lagrangian multipliers. It is worth mentioning that the deliverability of flexible resources will result in congestion components in marginal prices. When the energy loss is ignored, the prices consist of the Lagrangian multipliers for the energy balance constraints and transmission line constraints. This author, Ge, Shahidehpour, and Li have done some work on pricing scheme with non-dispatchable renewables [22], [26]. The principles in [22] are applicable to the model in this work where the curtailment of VER generation is considered. For example, the definition of Uncertainty Marginal Price can be extended to the marginal price for flexibility. Interested readers are referred to [22], [26] for details. With the fair treatment for uncertainty and flexibility, VERs incline to purchase flexibility cost-effectively. That requires VERs to self-manage uncertainties or self-optimize their resources. In return, the

flexibility demand (or uncertainty level) can be reduced from the system's point of view. Two questions are of great interest in future: what is the best bidding strategy for VER? How can flexibility demand be aggregated with uncertainty correlations information? With the distribution information, the expected cost can also be employed in the objective function.

REFERENCES

[1] "Electric power annual 2015," U.S. Energy Information Administration, Tech. Rep., Nov. 2016.

[2] X. Guan, P. B. Luh, H. Yan, and J. Amalfi, "An optimization-based method for unit commitment," *Int. J. Electr. Power & Energy Syst.*, vol. 14, no. 1, pp. 9–17, Feb. 1992.

[3] M. Shahidehpour, H. Yamin, and Z. Li, *Market operations in electric power systems*. New York, NY, USA: Wiley-IEEE Press, 2002.

[4] S. Takriti, J. Birge, and E. Long, "A stochastic model for the unit commitment problem," *IEEE Trans. Power Syst.*, vol. 11, no. 3, pp. 1497–1508, Aug. 1996.

[5] L. Wu, M. Shahidehpour, and T. Li, "Stochastic security-constrained unit commitment," *IEEE Trans. Power Syst.*, vol. 22, no. 2, pp. 800–811, May 2007.

[6] J. M. Morales, A. J. Conejo, and J. Perez-Ruiz, "Economic valuation of reserves in power systems with high penetration of wind power," *IEEE Trans. Power Syst.*, vol. 24, no. 2, pp. 900–910, May 2009.

[7] R. Jiang, J. Wang, and Y. Guan, "Robust unit commitment with wind power and pumped storage hydro," *IEEE Trans. Power Syst.*, vol. 27, no. 2, pp. 800–810, May 2012.

[8] D. Bertsimas, E. Litvinov, X. Sun, J. Zhao, and T. Zheng, "Adaptive robust optimization for the security constrained unit commitment problem," *IEEE Trans. Power Syst.*, vol. 28, no. 1, pp. 52–63, Feb. 2013.

[9] D. Bienstock, M. Chertkov, and S. Harnett, "Chance-constrained optimal power flow: Risk-aware network control under uncertainty," *SIAM Review*, vol. 56, no. 3, pp. 461–495, Jan. 2014.

[10] J. Warrington, P. Goulart, S. Mariethoz, and M. Morari, "Policy-based reserves for power systems," *IEEE Trans. Power Syst.*, vol. 28, no. 4, pp. 4427–4437, Nov. 2013.

[11] R. A. Jabr, "Adjustable robust OPF with renewable energy sources," *IEEE Trans. Power Syst.*, vol. 28, no. 4, pp. 4742–4751, Nov. 2013.

[12] A. Charnes, W. W. Cooper, and G. H. Symonds, "Cost horizons and certainty equivalents: an approach to stochastic programming of heating oil," *Management Science*, vol. 4, no. 3, pp. 235–263, Apr. 1958.

[13] B. Wollenberg and A. Wood, *Power generation, operation and control*. Hoboken, NJ, USA: John Wiley & Sons, 1996.

[14] R. Tanabe, K. Yasuda, R. Yokoyama, and H. Sasaki, "Flexible generation mix under multi objectives and uncertainties," *IEEE Trans. on power syst.*, vol. 8, no. 2, pp. 581–587, May 1993.

[15] Y. V. Makarov, C. Loutan, J. Ma, and P. d. Mello, "Operational impacts of wind generation on California power systems," *IEEE Trans. Power Syst.*, vol. 24, no. 2, pp. 1039–1050, May 2009.

[16] D. S. Kirschen, J. Ma, V. Silva, and R. Belhomme, "Optimizing the flexibility of a portfolio of generating plants to deal with wind generation," in *IEEE PES General Meeting*, Detroit, MI, USA, Jul. 2011, pp. 1–7.

[17] J. Ma, V. Silva, R. Belhomme, D. S. Kirschen, and L. F. Ochoa, "Evaluating and planning flexibility in sustainable power systems," *IEEE Trans. Sust. Energy*, vol. 4, no. 1, pp. 200–209, Jan 2013.

[18] J. B. Cardell and C. L. Anderson, "A flexible dispatch margin for wind integration," *IEEE Trans. Power Syst.*, vol. 30, no. 3, pp. 1501–1510, May 2015.

[19] R. Chen, J. Wang, A. Botterud, and H. Sun, "Wind power providing flexible ramp product," *IEEE Trans. Power Syst.*, vol. 32, no. 3, pp. 2049–2061, May 2017.

[20] M. A. Bucher, S. Chatzivasileiadis, and G. Andersson, "Managing flexibility in multi-area power systems," *IEEE Trans. Power Syst.*, vol. 31, no. 2, pp. 1218–1226, Mar. 2016.

[21] H. Ye, Y. Ge, M. Shahidehpour, and Z. Li, "Pricing energy and flexibility in robust security-constrained unit commitment model," in *IEEE PES General Meeting*, Boston, MA, USA, Jul. 2016, pp. 1–5.

[22] H. Ye, Y. Ge, M. Shahidehpour, and Z. Li, "Uncertainty marginal price and day-ahead market clearing for energy, uncertainty, generation and transmission reserves with robust unit commitment," *IEEE Trans. Power Syst.*, vol. 32, no. 3, pp. 1782–1795, May 2017.

[23] J. Zhao, T. Zheng, and E. Litvinov, "Variable resource dispatch through do-not-exceed limit," *IEEE Trans. Power Syst.*, vol. 30, no. 2, pp. 820–828, Mar. 2015.

[24] W. Wei, J. Wang, and S. Mei, "Dispatchability maximization for co-optimized energy and reserve dispatch with explicit reliability guarantee," *IEEE Trans. Power Syst.*, vol. 31, no. 4, pp. 3276–3288, Jul. 2016.

[25] F. Qiu, Z. Li, and J. Wang, "A data-driven approach to improve wind dispatchability," *IEEE Trans. Power Syst.*, vol. 32, no. 1, pp. 421–429, Jan. 2017.

[26] H. Ye and Z. Li, "Deliverable robust ramping products in real-time markets," *IEEE Trans. Power Syst.*, vol. 33, no. 1, pp. 5–18, Jan. 2018.

[27] H. Ye, J. Wang, Y. Ge, J. Li, and Z. Li, "Robust integration of high-level dispatchable renewables in power system operation," *IEEE Trans. Sust. Energy*, vol. 31, no. 5, pp. 3527–3536, Sept. 2016.

[28] E. Litvinov, F. Zhao, and T. Zheng, "Alternative auction objectives and pricing schemes in short-term electricity markets," in *IEEE PES General Meeting*, Calgary, AB, CA, Jul. 2009, pp. 1–11.

[29] A. Somani and L. Tesfatsion, "An agent-based test bed study of wholesale power market performance measures," *IEEE Comput. Intell. Mag.*, vol. 3, no. 4, pp. 56–72, Nov. 2008.

[30] L. Xu and D. Tretheway, "Flexible ramping product-revised straw proposal," Tech. Rep., 2015, [Accessed on: Jul. 1, 2015]. [Online]. Available: http://www.caiso.com/Documents/DraftTechnicalAppendix_FlexibleRampingProduct.pdf

[31] MISO, "Ramp product questions and answers," 2016, accessed on: Dec. 30, 2016. [Online]. Available: https://www.misoenergy.org/Library/Repository/Communication%20Material/Strategic%20Initiatives/Ramp%20Product%20Questions%20and%20Answers.pdf

[32] A. Ben-Tal, A. Goryashko, E. Guslitzer, and A. Nemirovski, "Adjustable robust solutions of uncertain linear programs," *Math. Program.*, vol. 99, no. 2, pp. 351–376, Mar 2004.

[33] H. Ye and Z. Li, "Robust security-constrained unit commitment and dispatch with recourse cost requirement," *IEEE Trans. Power Syst.*, vol. 31, no. 5, pp. 3527–3536, Sept. 2016.

[34] S. Boyd and L. Vandenberghe, *Convex optimization*. Cambridge, U.K.: Cambridge University Press, 2009.

[35] A. Ben-Tal and A. Nemirovski, "Robust solutions of uncertain linear programs," *Oper. Res. Lett*, vol. 25, no. 1, pp. 1–13, Aug. 1999.

[36] X. Zhao, P. B. Luh, and J. Wang, "Surrogate gradient algorithm for lagrangian relaxation," *J. Optim. Theory Appl.*, vol. 100, no. 3, pp. 699–712, Mar. 1999.

[37] X. Chen and Y. Zhang, "Uncertain linear programs: extended affinely adjustable robust counterparts," *Oper. Res.*, vol. 57, no. 6, pp. 1469–1482, Dec. 2009.

[38] A. Lorca, A. Sun, E. Litvinov, and T. Zheng, "Multistage adaptive robust optimization for the unit commitment problem," *Oper. Res.*, vol. 64, no. 1, pp. 32–51, Jan. 2016.

[39] H. Ye and Z. Li, "Necessary conditions of line congestions in uncertainty accommodation," *IEEE Trans. Power Syst.*, vol. 31, no. 5, pp. 4165–4166, Sept. 2016.

Hongxing Ye (SM'17) received his B.S. degree in Information Engineering, in 2007, and M.S. degree in Systems Engineering, in 2011, both from Xi'an Jiaotong University, China, and the Ph.D. degree in Electrical Engineering from the Illinois Institute of Technology, Chicago, in 2016. He is currently an Assistant Professor in the Department of Electrical Engineering and Computer Science at Cleveland State University. His research interests include large-scale optimization in power systems, electricity market, renewable integration, and cyber-physical system security in smart grid. He was honored "Outstanding Reviewer" for IEEE Transactions on Power Systems and IEEE Transactions on Sustainable Energy. He received Sigma Xi Research Excellence Award at Illinois Institute of Technology in 2016.